

**ORBIT-RADIAL CONTROL OF A TWO-CRAFT  
COULOMB FORMATION ABOUT CIRCULAR  
ORBITS AND LIBRATION POINTS**

**Ravi Inampudi and Hanspeter Schaub**

**4th International Conference on  
Spacecraft Formation Flying  
Missions & Technologies**

St-Hubert, Québec

May 18–20, 2011

# Orbit-Radial Control of a Two-Craft Coulomb Formation about Circular Orbits and Libration Points

Ravi Inampudi\* and Hanspeter Schaub†

This paper investigates the orbit radial stabilization of a 2-craft virtual Coulomb structure about circular orbits and at Earth-Moon libration points. A generic Lyapunov feedback controller is designed for asymptotically stabilizing an orbit radial configuration about circular orbits and collinear libration points. The new feedback controller at the libration points is provided as a generic control law in which circular Earth orbit control form a special case. This control law can withstand differential solar perturbation effects on the two-craft formation. Electrostatic Coulomb forces acting in the longitudinal direction control the relative distance between the two satellites and inertial electric propulsion thrusting acting in the transverse directions control the in-plane and out-of-plane attitude motions. The electrostatic virtual tether between the two craft is capable of both tensile and compressive forces. Using the Lyapunov's second method the feedback control law guarantees closed loop stability. Numerical simulations using the non-linear control law are presented for circular orbits and at an Earth-Moon collinear libration point.

## I. Introduction

In the presence of differential solar radiation pressure effects, this paper investigates the application of non-linear control techniques in stabilizing a two-craft formation virtually connected by an electrostatic (Coulomb) force. The basic idea of Coulomb propulsion of free-flying vehicles is to control the spacecraft formation shape and size using the inter-spacecraft forces created by electrostatically charging the spacecraft to different potentials.<sup>1,2</sup> For tight formation control of spacecraft separation distances on the order of 100 metres or less, this propellant-less thrusting is an attractive solution over conventional electric propulsion or chemical thrusting which can cause thruster plume contamination of the neighbouring spacecraft. Coulomb propulsion has several advantages: it is a highly efficient system with a renewable energy source with  $I_{sp}$  values ranging up to  $10^{13}$  seconds, it requires very little electrical power requirements (one Watt or less), and it has a very high bandwidth for relative motion control with charge transition times on the order of milli-seconds.<sup>1</sup> These advantages enable high precision, close-proximity formation flying with several potential applications in space technologies such as high accuracy wide-field-of-view optical interferometry missions, spacecraft cluster control, as well as rendezvous and docking maneuvers. Coulomb propulsion has its drawbacks. The formation dynamics are highly coupled and non-linear and Coulomb formation flying concept is feasible in less dense plasma environments at geostationary orbit (GEO) altitudes or higher. Moreover, as the electrostatic forces are internal to the formation, Coulomb forces cannot be used to reorient a full formation to a new orientation and external forces such as thrusters or differential gravity gradient torques must be used.

In 2002, Parker and King presented the Coulomb propulsion concept to control a cluster of free-flying spacecraft in References 1 and 2. They present analytic solutions for Hill-frame invariant three and five-craft

---

\*Graduate Student, Aerospace Engineering Sciences Department, University of Colorado, Boulder, CO. AIAA Member

†Associate Professor, H. Joseph Smead Fellow, Aerospace Engineering Sciences Department, University of Colorado, Boulder, CO. AIAA Associate Fellow

static Coulomb formations with symmetry assumptions. The pre-defined craft locations in the formation and constant charges in the rotating Hill frame perfectly cancel all relative motion of the charged spacecraft. References 3–5 present more systematic analytic solutions for two, three, and four-spacecraft formations and demonstrate numerically possible formations with as many as 9 craft in GEO orbits. The open-loop static Coulomb formations are all numerically unstable. Reference 6 formulates necessary conditions to achieve such static Coulomb formations with constant charges. Reference 7 present closed-loop feedback stabilized virtual Coulomb structure solutions for in-orbit two-craft configurations (radial, along-track and orbit normal). For an orbit radial Coulomb tether configuration, a charge feedback law stabilize the relative distance between the satellites exploiting the differential gravitational attraction to stabilize the in-plane attitude motion. Along the orbit-normal and the along-track directions, to asymptotically stabilize the satellite formation shape and attitude, the authors present hybrid feedback control laws which combine conventional thrusters and Coulomb forces. Furthermore, Reference 7 investigates the linear dynamics and stability analysis of expansion and contraction reconfiguration maneuvers for all three equilibrium configurations using linearized time-varying dynamical models. In such reconfiguration maneuvers, stability regions limit the Coulomb tether expansion and contraction rates.

Tether formations at the libration points are useful for remote sensing missions to establish a long-baseline imaging capability or to ensure better stationkeeping configurations. Reference 8 considers the equilibrium configurations of a rigid tethered system near all five libration points and carries out the stability analysis when it is near the translunar libration point. Also, the NIAC report in Reference 1 analyzes the suitability of Coulomb control for a static collinear five-vehicle formation at Earth-Sun Lagrange points where the formation local dynamics ignore gravity. Furthermore, Reference 9 presents compatibility results of using Coulomb satellites with electric propulsion and autonomous path planning techniques at the libration points for formation keeping and reconfiguration of swarms of satellites. At Geostationary Orbits (GEO) the Debye length varies between 80-1400 m, with a mean of about 180 m which constrains the maximum possible formation length.<sup>10</sup> In the interplanetary space at Earth-moon libration points, the Debye length varies between 10-40 m.<sup>1,11</sup> But despite the low value of the Debye length, multi-craft equilibrium formations are reported to exist at the Earth-Sun  $L_1$  Lagrange point.<sup>9</sup> Furthermore, as a consequence of discussions in Reference 12, the effective Debye lengths in deep space still yield charged relative motion dynamics that are primarily influenced through classical electrostatics. Reference 13 shows that for a two spacecraft Coulomb formation at the gravitational three-body libration points, three equilibrium configurations exist (radial, along-track and orbit normal). And Reference 14 present the linearized radial, along-track and orbit-normal dynamics and stability of a 2-craft Coulomb tether formation at Earth-Moon libration points. The assumption for the linearized study is that the sunlit areas of the two-craft are equal such that the differential solar radiation pressure on the formation is zero.

Differential solar drag is the largest disturbance acting on a tether formation at GEO and at libration points (Sun-Earth or Earth-Moon).<sup>10,11</sup> For example, on a typical micro-craft in Earth orbit the maximum solar torque magnitude of about  $10^{-5}$  Nm is essentially constant with orbit altitude.<sup>15</sup> The gravity gradient torque is inversely proportional to the orbit radius cubed, but in low orbits has a maximum magnitude on the order of solar torque, and above an altitude of about 20,000 kilometers it becomes relatively insignificant (less than 1%).<sup>15</sup> Therefore, at libration point distances, in the presence of a differential solar drag on the formation, the gravity gradient torques may no longer be sufficient to stabilize the in-plane motion of a 2-craft virtual Coulomb structure in the radial equilibrium position. Moreover, in the presence of differential solar drag on a two craft Coulomb formation in circular orbits, Reference 7 shows that the states are bounded with the charge feedback law. These limitations motivate us to study the non-linear dynamics and stability analysis of an orbit-radial two-craft Coulomb formation about circular orbits and at Earth-Moon libration points.

References 16 and 17 use a Lyapunov approach for tether deployment and retrieval in circular orbits. In their study, tether mass and flexibility, solar radiation pressure as well as aerodynamic effects are neglected. The Lyapunov feedback control method use a Lyapunov function based on a first integral of motion of the dynamical system. The control laws are simple and utilize tether tension control as well as out-of-plane thrusting. In this paper, a similar approach is taken to stabilize the formation shape and size in circular orbits and at the libration points in the presence of differential solar radiation pressure affects. The goal is to design a generic Lyapunov feedback controller that can withstand differential solar perturbation effects and to asymptotically stabilize an orbit radial 2-craft Coulomb structure about circular orbits and collinear

libration points. First the generic non-linear equations of motion for a two spacecraft Coulomb formation at the libration points are presented. This general framework for two-craft dynamics at the collinear libration points present circular Earth orbit dynamics as a special case. Then the environmental torques due to gravity gradient forces and solar radiation pressure affects at GEO and at Earth-Moon libration points are discussed. Of interest is to study if the gravity gradient forces on a radial equilibrium two-craft Coulomb tether formation are sufficient to withstand the differential solar drag affects. Numerical results show the gravity gradient and differential solar drag force magnitudes on the formation. Finally, a generic controller is designed that can withstand differential solar perturbation effects in orbit radial configuration about circular orbits and at Earth-Moon collinear libration points. Numerical simulations validate the Lyapunov controller performance.

## II. Equations of Motion - Circular Orbits and Collinear Libration Points

The equations of motion for a two spacecraft Coulomb formation at collinear Earth-Moon libration points are derived in Reference 14. They are presented here incorporating the differential solar radiation pressure perturbations. Defining  $L$  to be the distance between the two satellites and  $L_{\text{ref}}$  the reference separation distance, the nondimensional separation distance variable  $l$  is set to  $\frac{L}{L_{\text{ref}}}$ . The nondimensional time variable is  $\tau = \Omega t$  where  $\Omega$  is the constant angular velocity of the Earth-Moon barycenter. And assuming  $f_{d\theta}$ ,  $f_{d\psi}$  and  $f_{dl}$  to be the non-dimensional differential solar perturbations in body frame, the non-linear equations governing the roll angle  $\theta$  out of the orbital plane, the pitch angle  $\psi$  in the orbital plane, and the separation distance  $l$  are

$$\theta'' + 2\frac{l'}{l}\theta' + \cos\theta \sin\theta((1 + \psi')^2 + 3\sigma \cos^2\psi) = \frac{u_\theta}{l} + \frac{f_{d\theta}}{l} \quad (1a)$$

$$\psi'' \cos^2\theta - 2\cos\theta(1 + \psi')(\theta' \sin\theta - \frac{l'}{l}\cos\theta) + 3\sigma \cos^2\theta \sin\psi \cos\psi = \frac{u_\psi}{l} + \frac{f_{d\psi}}{l} \quad (1b)$$

$$l'' - l(\theta'^2 + (1 + \psi')^2 \cos^2\theta - \sigma(1 - 3\cos^2\theta \cos^2\psi)) = -u_l - f_{dl} \quad (1c)$$

where the prime denotes the derivative with respect to non-dimensional time. And  $u_l$ ,  $u_\psi$  and  $u_\theta$  are the non-dimensional body frame control variables. The control variable  $u_l$  is associated with Coulomb propulsion, and  $u_\psi$  and  $u_\theta$  are related to electric propulsion. The equations of motion are coupled non-linear ordinary differential equations that define the motion of a two-craft Coulomb formation at any of the three collinear Lagrangian points. The parameter  $\sigma$  is a positive constant that depends on the collinear Lagrangian point ( $L_1$ ,  $L_2$ ,  $L_3$ ) under consideration. It is defined as

$$\sigma = \frac{1 - \nu}{|\frac{r_{x_0}}{d} + \nu|^3} + \frac{\nu}{|\frac{r_{x_0}}{d} - 1 + \nu|^3} > 0 \quad (2)$$

where  $\nu = \frac{M_2}{M_1 + M_2}$  and  $1 - \nu = \frac{M_1}{M_1 + M_2}$  with  $M_1$  and  $M_2$  being the dominant masses of the two gravitational primaries, Earth and Moon. And  $d$  is the distance between the two primaries with  $r_{x_0}$  being the  $x$  position of a collinear libration point with respect to the barycenter.

Interestingly, for " $\sigma = 1$ ", the equations turn out to be the same equations that were found in Reference 7 for orbit radial 2-craft formation at GEO. Thus, the non-linear equations of motion about orbit radial equilibrium in Eqs. (1) form a general framework that covers both circular GEO and colinear libration point departure motion. By changing the constant  $\sigma$  either motion is described.

If the two-craft formation is aligned in the radial direction, the formation remains statically fixed relative to the rotating orbiting frame  $\mathcal{O}$  provided the non-linear equations Eq. (1) satisfy the following radial equilibrium conditions

$$\theta = \theta' = \theta'' = \psi = \psi' = \psi'' = l' = l'' = 0 \quad \text{and} \quad l = 1 \Rightarrow L = L_{\text{ref}} \quad (3)$$

Eq. (1c) provides the nominal product of charges  $Q_{\text{ref}} = q_1 q_2$  needed to achieve this static Coulomb formation as<sup>14</sup>

$$Q_{\text{ref}} = -(2\sigma + 1)\Omega^2 \frac{L^3}{k_c} \frac{m_1 m_2}{m_1 + m_2} \quad (4)$$

Thus, the satellites appear frozen with respect to the rotating frame when the charge product  $Q_{\text{ref}}$  satisfies Eq. (4). Since the charge product term is negative it implies that the spacecraft charges will have opposite charge signs and also, an infinite number of charge pairs can satisfy  $Q_{\text{ref}} = q_1 q_2$ . Although unequal charges are possible between the two crafts, in this study, the charge magnitudes are set equal.

### III. Environmental Torques - GEO and Libration Points

This section discusses environmental torques due to gravity gradient and solar radiation pressure effects on a two-craft formation. The gravity gradient torque expressions and solar radiation pressure models at GEO and at Earth-Moon libration points are presented. To study whether the gravity gradient forces on a radial equilibrium two-craft Coulomb tether formation are sufficient to withstand the solar drag affects, the magnitudes of gravity gradient forces at GEO heights and libration point distances are compared against the differential solar drag forces on the formation. Numerical results show the gravity gradient and differential solar drag force magnitudes on the formation at GEO and at Earth-Moon libration points.

#### A. Gravity Gradient Torques

The gravity gradient torque expression at GEO is obtained from<sup>18</sup>

$${}^{\mathcal{B}}\mathbf{L}_G = \begin{bmatrix} L_{G_1} \\ L_{G_2} \\ L_{G_3} \end{bmatrix} = \frac{3GM_e}{r_c^5} \begin{bmatrix} r_{c2}r_{c3}(I_{33} - I_{22}) \\ r_{c1}r_{c3}(I_{11} - I_{33}) \\ r_{c1}r_{c2}(I_{22} - I_{11}) \end{bmatrix} \quad (5)$$

where  $r_{c1}$ ,  $r_{c2}$  and  $r_{c3}$  are the  $\mathcal{B}$  frame components of a two-craft formation center of mass position vector  $\mathbf{r}_c$  in GEO.  $G$  is the gravity constant and  $M_e$  is the mass of the planet Earth. The body frame inertia matrix of a two-craft formation in radial equilibrium is<sup>7</sup>

$${}^{\mathcal{B}}[I] = \begin{bmatrix} 0 & 0 & 0 \\ 0 & I & 0 \\ 0 & 0 & I \end{bmatrix} \quad (6)$$

where  $I = \frac{m_1 m_2}{m_1 + m_2} L^2$  and  $m_1$ ,  $m_2$  are the masses of the two spacecraft.

Using Eq. (5), the gravity gradient torque of a radial equilibrium two-craft Coulomb tether formation at GEO becomes

$${}^{\mathcal{B}}\mathbf{L}_G = 3\Omega^2 \begin{bmatrix} 0 \\ -I \cos \theta \sin \theta \cos^2 \psi \\ -I \cos \theta \cos \psi \sin \psi \end{bmatrix} \quad (7)$$

where  $\Omega^2 = \frac{\mu}{r_c^3}$  with  $\mu = GM_e$ .

Similarly, the gravity gradient torque expression at libration points is

$${}^{\mathcal{B}}\mathbf{L}_G = \begin{bmatrix} L_{G_1} \\ L_{G_2} \\ L_{G_3} \end{bmatrix} = \frac{3GM_1}{r_c^5} \begin{bmatrix} r_{c2}r_{c3}(I_{33} - I_{22}) \\ r_{c1}r_{c3}(I_{11} - I_{33}) \\ r_{c1}r_{c2}(I_{22} - I_{11}) \end{bmatrix} + \frac{3GM_2}{r_c'^5} \begin{bmatrix} r_{c2}'r_{c3}'(I_{33} - I_{22}) \\ r_{c1}'r_{c3}'(I_{11} - I_{33}) \\ r_{c1}'r_{c2}'(I_{22} - I_{11}) \end{bmatrix} \quad (8)$$

where  $r_{c1}$ ,  $r_{c2}$ ,  $r_{c3}$  and  $r_{c1}'$ ,  $r_{c2}'$  and  $r_{c3}'$  are the  $\mathcal{B}$  frame components of a two-craft formation center of mass position vectors  $\mathbf{r}_c$  and  $\mathbf{r}_c'$  at a collinear libration point from the two primaries in the plane.

Using Eq. (8), the gravity gradient torque of a radial equilibrium two-craft Coulomb tether formation at a collinear libration point becomes

$${}^{\mathcal{B}}\mathbf{L}_G = 3(\Omega_1^2 + \Omega_2^2) \begin{bmatrix} 0 \\ -I \cos \theta \sin \theta \cos^2 \psi \\ -I \cos \theta \cos \psi \sin \psi \end{bmatrix} \quad (9)$$

where  $\Omega_1^2 = \frac{\mu_1}{r_c^3}$  and  $\Omega_2^2 = \frac{\mu_2}{r_c'^3}$  with  $\mu_1 = GM_1$  and  $\mu_2 = GM_2$ .

## B. Solar Radiation Pressure (SRP)

At GEO, the inertial acceleration vector  $\mathbf{a}_{\text{SRP}}$  in  $\text{m/s}^2$  due to the effects of solar radiation pressure (SRP) is given as<sup>7,19</sup>

$$\mathbf{a}_{\text{SRP}} = -\frac{C_r A F}{mc} \frac{\mathbf{r}}{\|\mathbf{r}\|^3} \quad (10)$$

where  $\mathbf{r}$  is the inertial position vector from the sun to the orbiting planet in AU,  $m$  is the mass of the spacecraft in kg, and  $A$  is the cross-sectional area of the spacecraft that is facing the sun in  $\text{m}^2$ . The constant  $F = 1372.5398 \text{ Watts/m}^2$  is the solar radiation flux,  $c = 299792458 \text{ m/s}$  is the speed of light, and  $C_r = 1.3$  is the radiation pressure coefficient. To compare the results at GEO from Reference 7, as shown

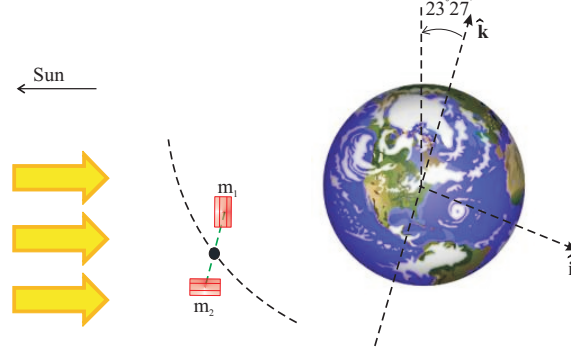


**Figure 1: Sun's Position and the Orientation of the Cylindrical Craft**

in Figure 1, the craft are modeled as cylinders of radius 0.5 m, height of 1 m and mass of 150 kg. For craft 1, the cylindrical surface with a square cross-sectional area of  $1 \text{ m}^2$  is constantly facing the sun, whereas for craft 2, it is the top of the cylinder with circular cross-sectional of  $0.25\pi \text{ m}^2$  that is facing the sun.

In the Earth-Moon system, the solar radiation pressure model is much different from that of the GEO environment. In the vicinity of the collinear libration points, the sun lines are treated as parallel lines. In order to describe the relative motion of the satellite with respect to the formation center of mass, a rotating Hill orbit frame  $\mathcal{O} : \{\hat{\mathbf{o}}_r, \hat{\mathbf{o}}_\theta, \hat{\mathbf{o}}_h\}$  whose origin coincides with the  $L_2$  libration point is chosen as shown in Figure 2. This rotating coordinate system orbits the Earth-Moon barycenter  $O$  with constant orbital angular velocity  $\Omega$ . In addition, the Earth-Moon system orbits the Sun with an angular velocity of  $\Omega_B$ . Consequently, the incident Sun line rotates in the orbit frame with a net angular velocity of  $\omega_s = \Omega - \Omega_B$ . A notable difference in the Earth-Moon system is that the direction of the incident sun line  $\mathbf{s}$  will vary continuously with respect to the  $\mathcal{O}$  frame as

$$\mathbf{s} = [\cos(\omega_s t), -\sin(\omega_s t), 0] \quad (11)$$

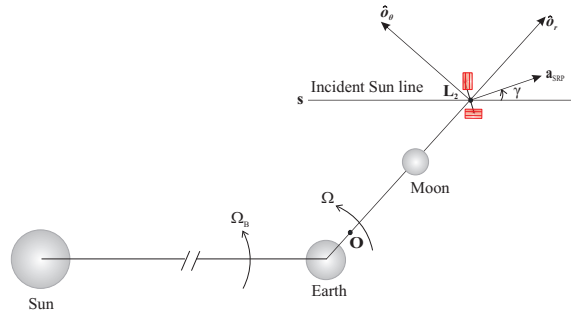


**Figure 2: Solar Radiation Pressure in the Vicinity of  $L_2$**

The solar torque on each craft depends on the orientation of the craft-normal relative to the orbit frame. The orientation of each craft with respect to the orbit frame is defined in terms of a cone angle  $\delta$  and a clock angle  $\gamma$ , as shown in Figure 3.<sup>19,20</sup> For this study, the cone and clock angles ( $\delta, \gamma$ ) for each craft are fixed.

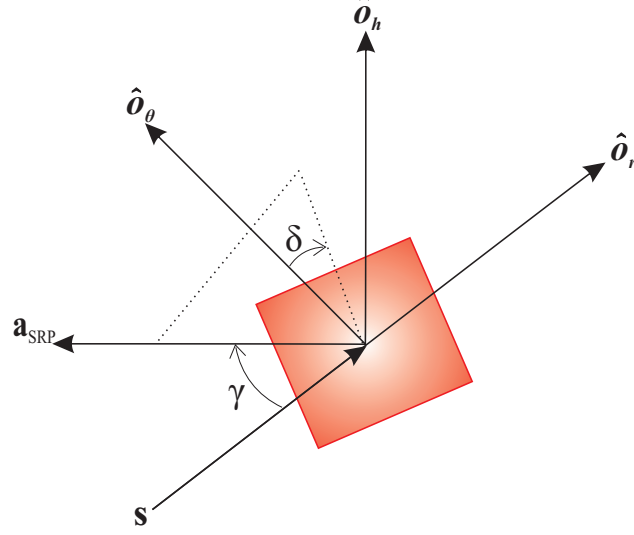


**Figure 3: Cone and Clock Angles of the Craft-normal relative to the Orbit Frame**

Therefore, the components of  $\mathbf{a}_{\text{SRP}}$  for a craft in the Earth-Moon orbit frame are given by<sup>19,20</sup>

$$a_{\text{SRPre}} = a_{\text{SRPmax}} \cos^2 \gamma \cos(\omega_s t - \gamma) \quad (12a)$$

$$a_{\text{SRPat}} = -a_{\text{SRPmax}} \cos^2 \gamma \sin(\omega_s t - \gamma) \sin \delta \quad (12b)$$

$$a_{\text{SRPon}} = a_{\text{SRPmax}} \cos^2 \gamma \sin(\omega_s t - \gamma) \cos \delta \quad (12c)$$

where  $a_{\text{SRPmax}} = |\mathbf{a}_{\text{SRP}}|$ ,  $a_{\text{SRPre}}$  is the component in orbit radial direction,  $a_{\text{SRPat}}$  is in the direction of orbital velocity (along-track), and the component  $a_{\text{SRPon}}$  is in the orbit normal direction. Eqs. (12) show that the SRP acceleration in the Earth-Moon system is periodic and time varying.

### C. Numerical Simulation

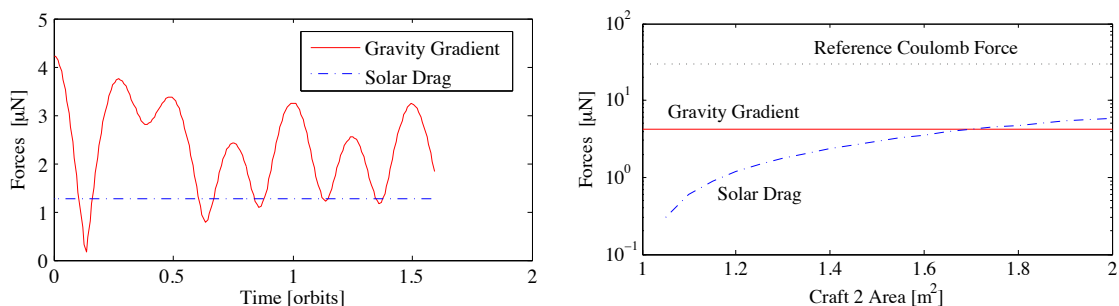
The solar drag and gravity gradient force magnitudes for nominal conditions are illustrated in the following numerical simulation. The simulation parameters and the values used are listed in Table 1.

**Table 1: Input Parameters Used in the Simulation**

Parameter	Value	Units
$m_1$	150	kg
$m_2$	150	kg
$L_{\text{ref}}$	25	m
$k_c$	$8.99 \times 10^9$	$\frac{\text{Nm}^2}{\text{C}^2}$
$\sigma$ (GEO)	1	
$\sigma$ (L <sub>2</sub> )	3.190432478	
$Q_{\text{ref}}$ (GEO)	-2.079105	$\mu\text{C}^2$
$Q_{\text{ref}}$ (L <sub>2</sub> )	-0.006816	$\mu\text{C}^2$
$\Omega$ (GEO)	$7.2915 \times 10^{-5}$	rad/sec
$\Omega$ (L <sub>2</sub> )	$2.661699 \times 10^{-6}$	rad/sec
$\delta L(0)$	0.5	m
$\psi(0)$	0.1	rad
$\theta(0)$	0.1	rad

Figure 4(a) shows the time histories of gravity gradient forces and differential solar drag on a two-craft formation in the GEO environment. For the nominal separation distance, the gravity gradient force is

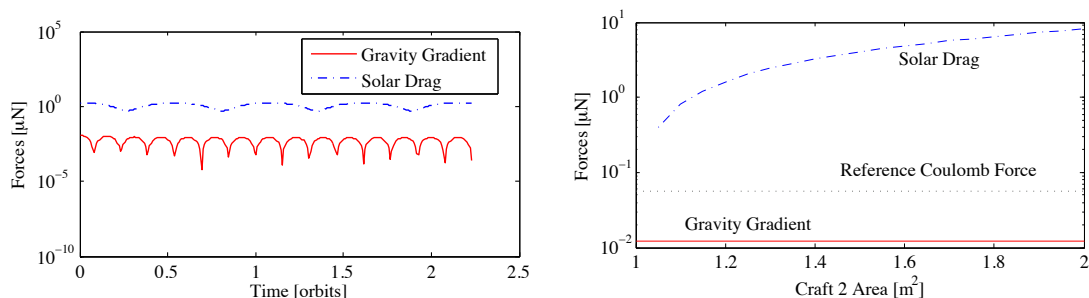
computed from the torque expression in Eq. (5) and the differential solar drag force is computed using Eq. (10). For craft 1, a square cross-sectional area of  $1 \text{ m}^2$  is constantly facing the sun, and, for craft 2, the circular cross-sectional area of  $0.25\pi \text{ m}^2$  is facing the sun. It clearly shows that the gravity gradient forces are sufficient to withstand the solar drag in the GEO environment. The results in Figure 4(b) are obtained by fixing the craft 1 cross-sectional area and varying the craft 2 cross-sectional area from  $1 \text{ m}^2$  to  $2 \text{ m}^2$ . These results indicate that even after increasing the solar drag, the combination of the maximum gravity gradient force and the reference Coulomb force magnitude obtained from Eq. (4) are sufficient to stabilize the formation.



a) Time Histories of Gravity Gradient and Solar Drag Forces    b) Force Magnitudes as a Function of Craft Area Ratio

**Figure 4: Radial Equilibrium Simulation Results at GEO for Nominal Initial Conditions**

Figure 5(a) shows the time histories of gravity gradient forces and differential solar drag for a two-craft formation at the Earth-Moon  $L_2$  libration point environment. It clearly shows that the gravity gradient forces are very weak, and thus cannot withstand the solar drag at  $L_2$ . The results in Figure 5(b) also indicate that the maximum gravity gradient force magnitude and the reference Coulomb force magnitude on each craft are not sufficient for stabilizing the formation. Therefore, unless equal sunlit surface areas of the two-craft are assumed such that the differential solar drag is zero, the charged feedback control law used in Reference 14 will not be able to stabilize the two-craft formation at the libration points. Consequently, for unequal sunlit surface areas of the two-craft a full state feedback control is required that uses larger Coulomb forces in the longitudinal direction and electric propulsion thrusters for transverse control.



a) Time Histories of Gravity Gradient and Solar Drag Forces    b) Force Magnitudes as a Function of Craft Area Ratio

**Figure 5: Radial Equilibrium Simulation Results at Earth-Moon  $L_2$  for Nominal Initial Conditions**

#### IV. Lyapunov Feedback Control

A generic controller is designed in this section that can withstand differential solar perturbation for orbit radial configuration about circular orbits and at Earth-Moon collinear libration points. Numerical simulations are shown to validate the controller performance.



## A. Feedback Control Development

Lyapunov's second method is used to develop a feedback control law for stabilizing a radial equilibrium two-craft Coulomb tether formation. The aim is to design a control law that takes into consideration constant solar radiation pressure effects at GEO as well as time varying solar radiation pressure disturbances at libration points. As presented in Reference 14, the kinetic energy for a two-craft Coulomb tether formation is not just a quadratic function of the velocities. Using the analytical approach discussed for the restricted three-body problem in Reference 21, the nondimensional Hamiltonian  $\hat{\mathcal{H}}$  for a two-craft tether formation in body coordinates is obtained as

$$\hat{\mathcal{H}} = \frac{1}{2}(l'^2 + l^2(\psi'^2 \cos^2 \theta + 3\sigma \cos^2 \theta \sin^2 \psi + \theta'^2 + (1 + 3\sigma) \sin^2 \theta - (1 + 2\sigma)) \quad (13)$$

where  $\sigma$  is a positive constant that depends on the collinear Lagrangian point chosen. For " $\sigma = 1$ ", the equation turns out to be the same equation that was found in Reference 16 for circular Earth orbits. Since the Lagrangian for a two-craft tether formation does not contain time explicitly,<sup>21</sup> it follows that the Hamiltonian is constant. Therefore, the two-craft Coulomb tether formation possesses a *Jacobi integral* in place of the energy integral as a constant of motion.

References 16 and 17 use the Hamiltonian as a Lyapunov function for stability analysis. Before the Hamiltonian is used as a Lyapunov function at libration points, its positive definiteness must be ascertained. Based on the constant of motion in Eq. (13), a Lyapunov function  $V_{\text{lyp}}$  is defined as

$$V_{\text{lyp}} = \frac{1}{2}(l'^2 + \tilde{K}_1(l - l_f)^2 + (\tilde{K}_2 + l^2)(\psi'^2 \cos^2 \theta + 3\sigma \cos^2 \theta \sin^2 \psi + \theta'^2 + (1 + 3\sigma) \sin^2 \theta)) \quad (14)$$

where  $l_f > 0$  is the desired final value of  $l$ ,  $\tilde{K}_1$  is a positive constant and  $\tilde{K}_2$  can either be positive or zero.  $V_{\text{lyp}}$  is clearly positive definite, and  $V_{\text{lyp}} = 0$  at the local radial equilibrium conditions in Eq. (3). Assuming  $f_{dl}$ ,  $f_{d\psi}$  and  $f_{d\theta}$  to be the non-dimensional differential solar perturbations in body frame, the time derivative of  $V_{\text{lyp}}$  is

$$V'_{\text{lyp}} = l'((1 + 2\sigma)l - u_l - f_{dl} + \tilde{K}_1(l - l_f)) - 2\frac{\tilde{K}_2}{l}(\psi'(1 + \psi')\cos^2 \theta + \theta'^2) + \theta'(\tilde{K}_2 + l^2)\left(\frac{u_\theta}{l} + \frac{f_{d\theta}}{l}\right) + \psi'(\tilde{K}_2 + l^2)\left(\frac{u_\psi}{l} + \frac{f_{d\psi}}{l}\right) \quad (15)$$

As mentioned before, the control variable  $u_l$  is associated with Coulomb propulsion acting in the longitudinal direction, and  $u_\psi$  and  $u_\theta$  utilize electric propulsion acting in the transverse directions.

The following control laws for  $u_l$ ,  $u_\psi$  and  $u_\theta$  can be selected

$$u_l = (1 + 2\sigma)l + \tilde{K}_1(l - l_f) - 2\frac{\tilde{K}_2}{l}(\psi'(1 + \psi')\cos^2 \theta + \theta'^2) + \tilde{K}_3 l' - f_{dl} \quad (16a)$$

$$u_\psi = -\tilde{K}_5 l \psi' - f_{d\psi} \quad (16b)$$

$$u_\theta = -\tilde{K}_4 l \theta' - f_{d\theta} \quad (16c)$$

where  $\tilde{K}_3$ ,  $\tilde{K}_4$  and  $\tilde{K}_5$  are positive constants.

Using these control laws, Eq. (15) leads to

$$V'_{\text{lyp}} = -\tilde{K}_3 l'^2 - (\tilde{K}_2 + l^2)(\tilde{K}_4 \theta'^2 + \tilde{K}_5 \psi'^2) \quad (17)$$

Proper choice of the gains guarantees the stability of the closed-loop system.

Substituting the control laws from Eq. (16) into the dynamics from Eqs. (1), the closed-loop system of

equations thus obtained are

$$\theta'' + 2\frac{l'}{l}\theta' + \cos\theta \sin\theta((1 + \psi')^2 + 3\sigma \cos^2\psi) + \tilde{K}_4\theta' = 0 \quad (18a)$$

$$\psi'' \cos^2\theta + 2\cos\theta(\frac{l'}{l}\cos\theta - \theta' \sin\theta)(1 + \psi') + 3\sigma \cos^2\theta \cos\psi \sin\psi + \tilde{K}_5\psi' = 0 \quad (18b)$$

$$l'' - l(\theta'^2 + (1 + \psi')^2 \cos^2\theta - \sigma(1 - 3\cos^2\theta \cos^2\psi)) + (1 + 2\sigma)l + \tilde{K}_1(l - l_f) - \frac{2\tilde{K}_2}{l}(\psi'(1 + \psi')\cos^2\theta + \theta'^2) + \tilde{K}_3l' = 0 \quad (18c)$$

These closed-loop system of equations can be used for three dimensional control of a 2-craft virtual Coulomb structure about circular orbits and at Earth-Moon libration points. Furthermore, they can be used either for station-keeping or for 2-craft expansion and contraction reconfigurations.

## B. Numerical Simulation

With the Lyapunov feedback law in Eq. (16), Figure 6 shows the simulation results in the GEO environment and Figure 7 shows the results at  $L_2$  libration point. The gain settings used for both the environments are  $\tilde{K}_1 = 2$ ,  $\tilde{K}_2 = 0$ ,  $\tilde{K}_3 = 4$ ,  $\tilde{K}_4 = 2$  and  $\tilde{K}_5 = 2$ . Figure 6(a) shows the Coulomb tether motion at GEO. The in-plane pitch motion  $\psi$ , out-of-plane motion  $\theta$ , and the separation distance deviation  $\delta L$  asymptotically converged to zero. The attitude motion converged in less than 0.5 orbits, whereas, the separation distance converged in about 1.3 orbits. Similar results are observed at  $L_2$  in Figure 7(a).

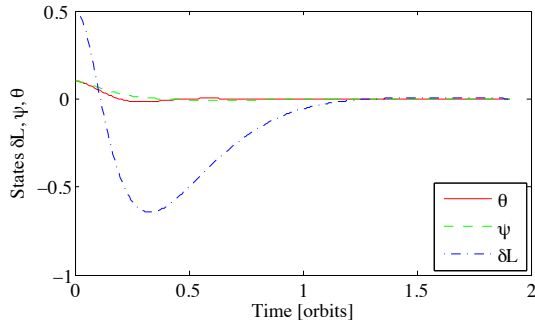
Figures 6(b) and 7(b) illustrate the spacecraft control charge  $q_1$  usage for the non-linear simulation. Because the solar drag perturbations on the two-craft formation exhibit cyclic behaviour as shown in Figure 6(c), the charge results depicted in Figure 6(b) also exhibit cyclic nature and do not converge to the static equilibrium reference value  $q_{1r}$ . The cyclic nature is more predominant at  $L_2$  in Figures 7(b) and 7(c). Furthermore, the micro-Coulomb charge requirements are easily realizable in practice. Figures 6(d) and 7(d) illustrate the Coulomb force utilization for longitudinal control and inertial thrusters usage for in-plane and out-of-plane control. Therefore, Coulomb control and transverse control (micro-thrusters) forces are on the order of micro-Newtons. Transverse control can be implemented either using Colloid or PPT micro-thrusters.

## V. Conclusion

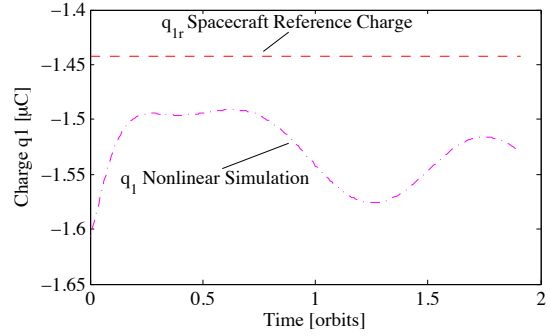
The stabilization of a two-craft Coulomb formation in the presence of differential solar drag is studied for orbit-radial equilibrium about circular orbits and at libration points. Previous research assumes that the two-craft areas exposed to sunlight are equal such that the differential solar radiation pressure is zero. This paper assumes that the differential solar drag on the two-craft formation is not zero. And in the presence of SRP disturbances, a Lyapunov feedback control method is presented for feedback stabilization of a radial equilibrium two-craft Coulomb tether formation about circular orbits and at libration points. The method uses a Lyapunov function based on a first integral of motion of the two-craft Coulomb formation. The controller designed using this method works very well and the control law utilizes a three-dimensional control (separation distance, in-plane and out-of-plane motion). The Lyapunov feedback control law obtained has a  $\sigma$  parameter which varies for each collinear libration point. Interestingly, setting " $\sigma = 1$ " yields a control law for orbit-radial equilibrium in Earth circular orbits. Therefore, the Lyapunov control law at the libration points is provided as a generic control law in which circular Earth orbit control forms a special case. In the numerical simulations, it is recommended that the control gains be chosen such that the pitch and roll angles do not exceed 90 degrees. This will ensure that undesirable equilibrium points are not reached. Depending on the desired final separation distance between the craft, the gains for the Coulomb propulsion control law should be appropriately adjusted. Assuming differential solar drag effects, numerical simulations are presented that illustrate the stabilization of a two-craft Coulomb formation in the GEO environment and at  $L_2$  libration point.

## References

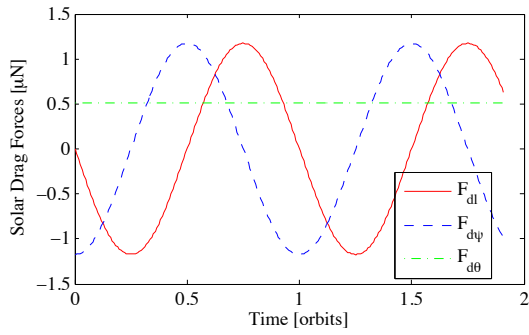
- <sup>1</sup>King, L. B., Parker, G. G., Deshmukh, S., and Chong, J.-H., "Spacecraft Formation-Flying using Inter-Vehicle Coulomb Forces," Tech. rep., NASA/NIAC, January 2002, <http://www.niac.usra.edu>.
- <sup>2</sup>King, L. B., Parker, G. G., Deshmukh, S., and Chong, J.-H., "Study of Interspacecraft Coulomb Forces and Implications for Formation Flying," *AIAA Journal of Propulsion and Power*, Vol. 19, No. 3, May/June 2003, pp. 497-505.



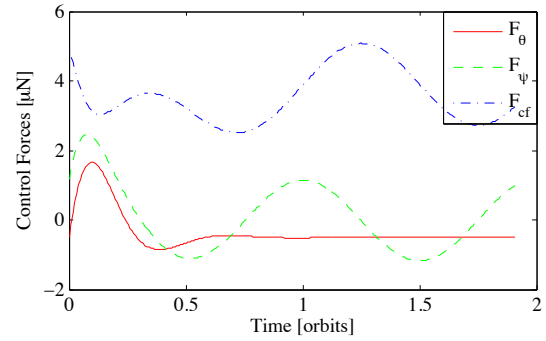
a) Time Histories of Length Variations  $\delta L$ , In-plane Pitch Angle  $\psi$ , and Out-of-plane Roll Angle  $\theta$



b) Spacecraft Charge Time Histories

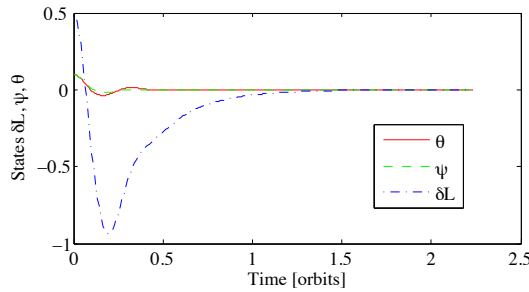


c) Solar Drag Perturbation Time Histories

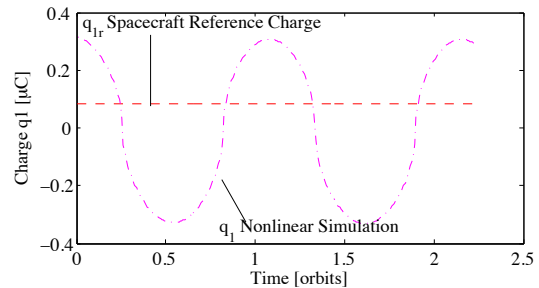


d) Control Time Histories

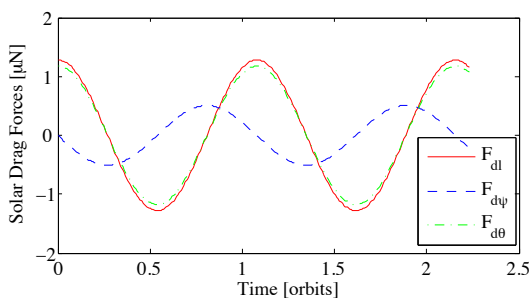
**Figure 6: Radial Equilibrium Nonlinear Control Simulation Results at GEO**



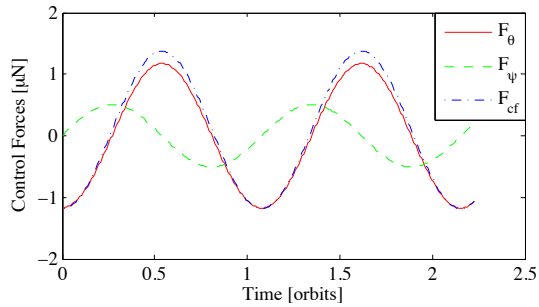
a) Time Histories of Length Variations  $\delta L$ , In-plane Pitch Angle  $\psi$ , and Out-of-plane Roll Angle  $\theta$



b) Spacecraft Charge Time Histories



c) Solar Drag Perturbation Time Histories



d) Control Time Histories

**Figure 7: Radial Equilibrium Nonlinear Control Simulation Results at  $L_2$**

- <sup>3</sup>Berryman, J., and Schaub, H., "Analytical Charge Analysis for 2- and 3-Craft Coulomb Formations," *AIAA Journal of Guidance, Control and Dynamics*, Vol. 30, No. 6, Nov.-Dec. 2007, pp. 1701-1710.
- <sup>4</sup>Vasavada, H., and Schaub, H., "Analytic Solutions for Equal Mass 4-Craft Static Coulomb Formation," *Journal of Astronautical Sciences*, Vol. 56, No. 1, January-March 2008, pp. 7-40.
- <sup>5</sup>Berryman, J., and Schaub, H., "Static Equilibrium Configurations in GEO Coulomb Spacecraft Formations," *AAS/AIAA Space Flight Mechanics Meeting*, Copper Mountain, CO, Jan. 23-27, 2005. Paper No. 05-104.
- <sup>6</sup>Schaub, H., Hall, C. D., and Berryman, J., "Necessary Conditions for Circularly-Restricted Static Coulomb Formations," *AAS Journal of Astronautical Sciences*, Vol 54, No. 3-4, July-Dec 2006, pp 525-541.
- <sup>7</sup>Natarajan, A., "A Study of Dynamics and Stability of Two-Craft Coulomb Tether Formations," *Ph.D. Dissertation*, Aerospace and Ocean Engineering Department, Virginia Polytechnic Institute and State University, Blacksburg, VA, May 2007.
- <sup>8</sup>Misra, A. K., Bellerose, J., and Modi, V. J., "Dynamics of a Tethered System near the Earth-Moon Lagrangian Points," *Proceedings of the 2001 AAS/AIAA Astrodynamics Specialist Conference*, Quebec City, Canada, Vol. 109 of Advances in the Astronautical Sciences, 2002, pp. 415-435.
- <sup>9</sup>Pettazzi, L., Krüger, H., Theil, S., and Izzo, D., "Electrostatic Forces for Satellite Swarm Navigation and Reconfiguration," *Technical Report*, ESA, Doc.No.: ARI-SS-FP-ZAR-001, 2006.
- <sup>10</sup>Romanelli, C. C., Natarajan, A., Schaub, H., Parker, G. G., and King, L. B., "Coulomb Spacecraft Voltage Study Due to Differential Orbital Perturbations," *AAS/AIAA Space Flight Mechanics Meeting*, Tampa Florida, January 22-26, 2006. Paper No. AAS 06-123.
- <sup>11</sup>Hastings, D., and Garrett, H., "Spacecraft-Environment Interactions," *Cambridge University Press*, 2004.
- <sup>12</sup>Murdoch, N., Izzo, D., Bombardelli, C., Carnelli, I., Hilgers, A., and Rodgers, D., "The Electrostatic Tractor for Asteroid Deflection," *58th International Astronautical Congress*, 2008, Paper IAC-08-A3.I.5.
- <sup>13</sup>Inampudi, R., and Schaub, H., "Two-Craft Coulomb Formation Relative Equilibria about Circular Orbits and Libration Points," *AAS/AIAA Space Flight Mechanics Meeting*, San Diego, CA, February 15-17, 2010, AAS Paper No. 10-163.
- <sup>14</sup>Inampudi, R., and Schaub, H., "Orbit Radial Dynamic Analysis of Two-Craft Coulomb Formation at Libration Points," *AAS/AIAA Astrodynamics Specialist Conference*, Toronto, Canada, Aug. 25, 2010. Paper No. AIAA-2010-7965.
- <sup>15</sup>Lawrence, D. A., and Whorton, M. S., "Solar Sail Dynamics and Coning Control in Circular Orbits," *Journal of Guidance, Control, and Dynamics*, Vol. 32, No. 3, May/June 2009, pp. 974-985.
- <sup>16</sup>Vadali, S. R., and Kim, E. S., "Feedback control of tethered satellites using Lyapunov stability theory," *Journal of Guidance, Control, and Dynamics*, Vol. 14, 1991, pp. 729-735.
- <sup>17</sup>Fujii, H. A., Uchiyama, K., and Kokubun, K., "Mission function control of tethered subsatellite deployment/retrieval: in-plane and out-of-plane motion," *Journal of Guidance, Control, and Dynamics*, Vol. 14, 1991, pp. 471-473.
- <sup>18</sup>Schaub, H., and Junkins, J. L., "Analytical Mechanics of Space Systems," *AIAA Education Series*, Reston, VA, 2003.
- <sup>19</sup>McInnes, C. R., "Solar Sailing: Technology, Dynamics and Mission Applications," *Springer-Praxis*, Chichester, UK, 1999.
- <sup>20</sup>Li, H., "Application of Solar Radiation Pressure to Formation Control near Libration Points," *Ph.D. Dissertation*, Department of Aerospace Engineering and Mechanical Engineering, University of Cincinnati, Ohio, Feb. 2008.
- <sup>21</sup>Meirovitch, L., "Methods of Analytical Dynamics," *Dover Publications, Inc*, Mineola, New York, 2003.